



Built-in electric field effect on the linear and nonlinear intersubband optical absorptions in InGaN strained single quantum wells

Yue-meng Chi, Jun-jie Shi *

State Key Laboratory for Mesoscopic Physics and Department of Physics, Peking University, Beijing 100871, PR China

ARTICLE INFO

Article history:

Received 3 January 2007

Received in revised form

8 April 2008

Accepted 5 May 2008

Available online 14 May 2008

PACS:

73.21.Fg

77.65.Ly

77.84.Bw

Keywords:

InGaN quantum wells

Built-in electric field

Linear and nonlinear intersubband optical absorptions

ABSTRACT

Considering the strong built-in electric field (BEF) induced by the spontaneous and piezoelectric polarizations and the intrasubband relaxation, we investigate the linear and nonlinear intersubband optical absorptions in $\text{In}_x\text{Ga}_{1-x}\text{N}/\text{Al}_y\text{Ga}_{1-y}\text{N}$ strained single quantum wells (QWs) by means of the density matrix formalism. Our numerical results show that the strong BEF is on the order of MV/cm, which can be modulated effectively by the In composition in the QW. This electric field greatly increases the electron energy difference between the ground and the first excited states. The electron wave functions are also significantly localized in the QW due to the BEF. The intersubband optical absorption peak sensitively depends on the compositions of In in the well layer and Al in the barrier layers. The intersubband absorption coefficient can be remarkably modified by the electron concentration and the incident optical intensity. The group-III nitride semiconductor QWs are suitable candidate for infrared photodetectors and near-infrared laser amplifiers.

© 2008 Elsevier B.V. All rights reserved.

1. Introduction

During the last couple of years, group-III nitride semiconductors have attracted much attention as materials for high-brightness light emitting diodes and laser diodes [1,2]. Such devices operate on the basis of the band to band (interband) transitions. However, due to the large conduction band offset, the III-nitride semiconductors low-dimensional heterostructures can also be designed to have transitions between the conduction subbands (intersubbands) with energy spacing in the near-infrared region [3,4]. Recently, the intersubband optical transition in III-nitride semiconductor quantum heterostructures has attracted much attention [5,6]. The ternary compound semiconductor heterostructures, such as InGaN/GaN, InGaN/AlGaIn and GaN/AlGaIn quantum wells (QWs), are all good candidates for some important optoelectronic devices, such as infrared photodetectors and waveguide switches working in the near-infrared range. Hence the intersubband optical transition in low-dimensional semiconductor heterostructures has always been a hot topic from both experiments [7–9] and theories [10,11] in recent years. In the present paper, we pay much attention to InGaN/AlGaIn QWs.

The group-III nitride semiconductors have large piezoelectric constants along the [0001] direction [12]. Considering the strain of the wurtzite InGaN/AlGaIn double heterostructure due to large lattice mismatch, the spontaneous and piezoelectric polarizations of the structure [13] can give rise to large polarization sheet charges on the interfaces or surfaces of the system, which, in turn, create a definite internal built-in electric field (BEF) inside the heterostructure. The intensity of the BEF can be estimated on the order of MV/cm [14] (see Fig. 1). A large dipole strength due to the BEF has been calculated [15]. It suggests that the intersubband optical transitions in the InGaN QWs have very large optical nonlinearity. These linear and nonlinear size-quantized intersubband optical transitions are interesting both for the fundamental investigation and for device applications, such as near-infrared laser amplifiers, photodetectors and high-speed electrooptical modulators [3,4,7]. To the best of our knowledge, there is little investigation for the linear and nonlinear intersubband optical absorptions in the important III-nitride QWs due to the strong BEF effect.

The paper is organized as follows. In Section 2, the BEF due to the piezoelectric and spontaneous polarizations in the InGaN/AlGaIn strained QWs is calculated. In Section 3, the electron states confined in InGaN/AlGaIn strained QWs are solved. In Section 4, the theoretical framework of the linear and nonlinear intersubband optical absorptions in the InGaN/AlGaIn QWs is outlined. Numerical results for the intersubband optical

* Corresponding author. Tel.: +86 10 62757594; fax: +86 10 62751615.
E-mail address: jjshi@pku.edu.cn (J.-j. Shi).

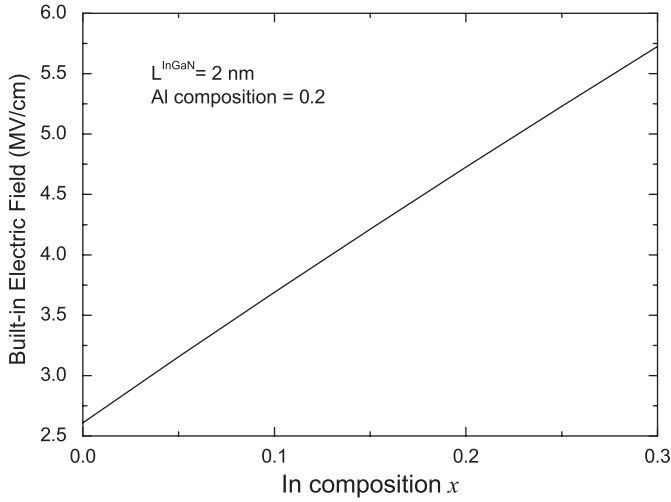


Fig. 1. Magnitude of the built-in electric field in the InGaN layer along the *c* axis as a function of the In composition for strained $\text{In}_x\text{Ga}_{1-x}\text{N}/\text{Al}_{0.2}\text{Ga}_{0.8}\text{N}$ QW with the well width $L^{\text{InGaN}} = 2$ nm.

absorptions are given and discussed in Section 5. Finally, we summarize the main conclusions obtained in this paper in Section 6.

2. BEF in strained group III nitride QWs

It has been known that both $\text{In}_x\text{Ga}_{1-x}\text{N}$ and $\text{Al}_y\text{Ga}_{1-y}\text{N}$ are wurtzite crystal structure, in which the chemical bonds between the neighboring atoms are not equivalent. This directly leads to a strong spontaneous polarization along the $[0001]$ direction [16]. The wurtzite crystal structure has also been found to have three independent nonvanishing component (e_{31}, e_{33}, e_{15}) of the piezoelectric tensor [16]. Therefore, the total zero-field macroscopic polarization \vec{P}_{tot} includes both the spontaneous polarization \vec{P}_{SP} in the equilibrium lattice and the strain-induced or piezoelectric polarization \vec{P}_{PE} .

For simplicity, we consider an $\text{In}_x\text{Ga}_{1-x}\text{N}/\text{Al}_y\text{Ga}_{1-y}\text{N}$ strained single QW with a thin $\text{In}_x\text{Ga}_{1-x}\text{N}$ layer sandwiched between two thick $\text{Al}_y\text{Ga}_{1-y}\text{N}$ layers grown along the $[0001]$ direction (*c*-axis) of the bulk materials denoted as the *z* direction. Following Takeuchi et al. [17], we ignore the complicated strains of the thick AlGaN layers due to the lattice and thermal mismatch of AlGaN and substrate (sapphire or SiC). The lattice constant *a* of the InGaN layer is reduced and *c* increased because of biaxial compressive stress. The total zero-field macroscopic polarization in the thick AlGaN layer is given by

$$\vec{P}_{\text{tot}}^{\text{AlGaN}} = \vec{P}_{\text{SP}}^{\text{AlGaN}} = P_{\text{SP}}^{\text{AlGaN}} \hat{z} \quad (1)$$

The total zero-field macroscopic polarization in the thin InGaN strained layer can be expressed as

$$\begin{aligned} \vec{P}_{\text{tot}}^{\text{InGaN}} &= \vec{P}_{\text{SP}}^{\text{InGaN}} + \vec{P}_{\text{PE}}^{\text{InGaN}} \\ &= P_{\text{SP}}^{\text{InGaN}} \hat{z} + [e_{31}(\varepsilon_{xx} + \varepsilon_{yy}) + e_{33}\varepsilon_{zz}] \hat{z} \end{aligned} \quad (2)$$

Here ε_{xx} , ε_{yy} , and ε_{zz} are the strain elements of the InGaN strained layer.

Considering the continuity of the electric displacement vector at the heterointerfaces of semiconductor QWs, we have

$$\begin{aligned} \varepsilon_e^{\text{AlGaN}} \varepsilon_0 F^{\text{AlGaN}} - \varepsilon_e^{\text{InGaN}} \varepsilon_0 F^{\text{InGaN}} \\ = P_{\text{SP}}^{\text{InGaN}} + P_{\text{PE}}^{\text{InGaN}} - P_{\text{SP}}^{\text{AlGaN}} \end{aligned} \quad (3)$$

where F^v ($v = \text{In}_x\text{Ga}_{1-x}\text{N}$ or $\text{Al}_y\text{Ga}_{1-y}\text{N}$) denotes the BEF of layer *v* and is caused by polarization of the QW structure, and ε_e^v is the electronic dielectric constant of the material *v*.

Based on Eq. (3) and the boundary condition that the potential energies on the far left and right of the QW structure are the same, we can obtain

$$\begin{aligned} F^{\text{InGaN}} &= \left| -\frac{P_{\text{SP}}^{\text{InGaN}} + P_{\text{PE}}^{\text{InGaN}} - P_{\text{SP}}^{\text{AlGaN}}}{\varepsilon_e^{\text{InGaN}} \varepsilon_0} \right| \\ F^{\text{AlGaN}} &\rightarrow 0 \end{aligned} \quad (4)$$

In general, the direction of the BEF in the InGaN layer depends on the orientation of the piezoelectric and spontaneous polarizations and can be determined by both the polarity of the crystal and the strain of the QW structure. For our $\text{Al}_y\text{Ga}_{1-y}\text{N}/\text{In}_x\text{Ga}_{1-x}\text{N}/\text{Al}_y\text{Ga}_{1-y}\text{N}$ strained single QW, the direction of the BEF is along the *z*-direction. Based on Eq. (4), we have calculated the strength of F^{InGaN} in the strained $\text{In}_x\text{Ga}_{1-x}\text{N}$ layer as a function of In composition. We can find from Fig. 1 that the BEF is extremely

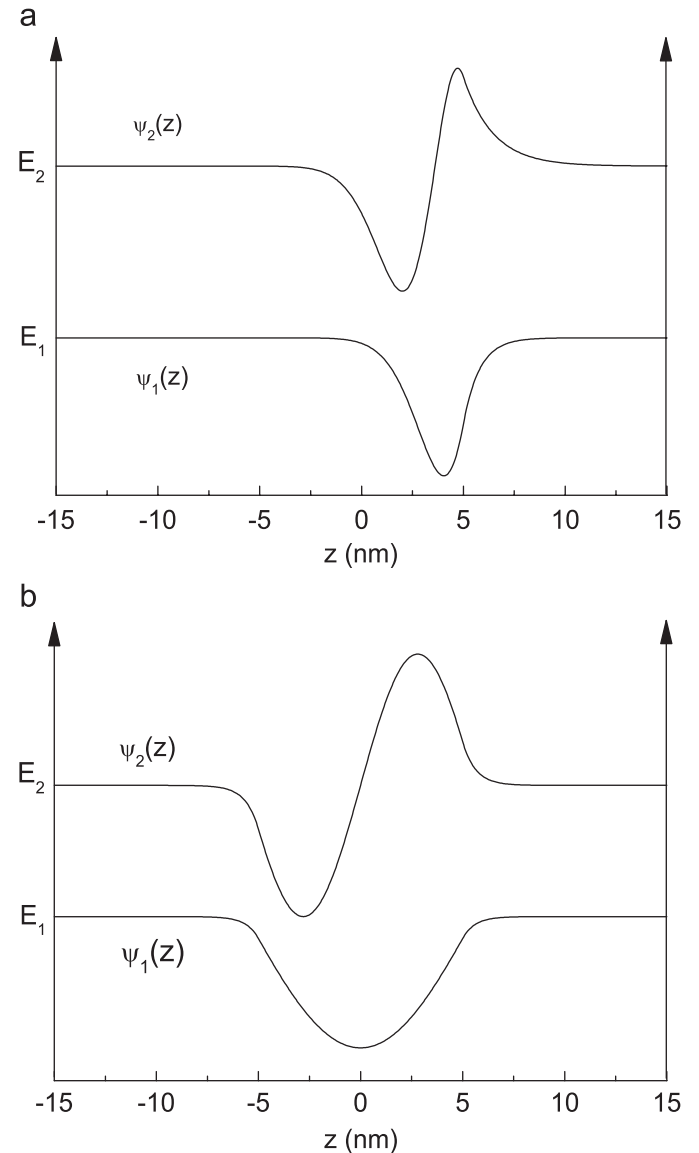


Fig. 2. Schematic diagrams of wave functions for an electron confined in a strained $\text{In}_x\text{Ga}_{1-x}\text{N}/\text{Al}_y\text{Ga}_{1-y}\text{N}$ QW with the two heterointerfaces located at $z = -5$ and 5 nm, respectively. Here the strong built-in electric field is included in (a) and ignored in (b).

strong, of the order of MV/cm. The increase of the In composition will enlarge the magnitude of the BEF in the InGaN strained layer.

Moreover, we can see from Fig. 2 that the strong BEF in the strained $\text{In}_x\text{Ga}_{1-x}\text{N}/\text{Al}_y\text{Ga}_{1-y}\text{N}$ QW can induce a remarkable change of the electron wave function spatial distribution. The electron wave functions are pushed to the right side of the QW, and the electrons are localized in the vicinity of the right interface of the QW due to the BEF. Moreover, we can also find from Fig. 2 that, compared with the case of ignoring the BEF, the energy separation between the ground and the first excited states increases if the BEF is included. The intersubband optical absorption peak will thus be significantly blue shifted by the BEF (refer to Fig. 4).

3. Electron states in strained InGaN single QWs

Let us now consider an electron confined in an $\text{In}_x\text{Ga}_{1-x}\text{N}/\text{Al}_y\text{Ga}_{1-y}\text{N}$ symmetric single QW with a well width L . Within the framework of the effective mass approximation, the electron Hamiltonian in the z direction can be written as

$$\hat{H} = -\frac{\hbar^2}{2m^*} \frac{d^2}{dz^2} + V(z) - eFz \quad (5)$$

where m^* and e denote the electron effective mass and the absolute value of the electron charge, respectively. $V(z)$ is the electron confined potential in the QW,

$$\alpha^{(3)}(\omega, I) = -\omega \sqrt{\frac{\mu}{\varepsilon_R}} \left(\frac{I}{2\varepsilon_0 n_r c} \right) \left(\frac{m^* k_B T}{L\pi\hbar^2} \right) \cdot \ln \left\{ \frac{1 + \exp[(E_F - E_1)/k_B T]}{1 + \exp[(E_F - E_2)/k_B T]} \right\} \cdot \frac{|M_{21}|^2 (\hbar/\tau_{in})}{[(E_2 - E_1 - \hbar\omega)^2 + (\hbar/\tau_{in})^2]} \cdot \left[4|M_{21}|^2 - \frac{|M_{22} - M_{11}|^2 \{(E_2 - E_1 - \hbar\omega)^2 - (\hbar/\tau_{in})^2 + 2(E_2 - E_1)(E_2 - E_1 - \hbar\omega)\}}{(E_2 - E_1)^2 + (\hbar/\tau_{in})^2} \right] \quad (17)$$

$$V(z) = \begin{cases} V_0, & |z| > L/2 \\ 0, & |z| \leq L/2 \end{cases} \quad (6)$$

Here V_0 is the potential height between $\text{In}_x\text{Ga}_{1-x}\text{N}$ and $\text{Al}_y\text{Ga}_{1-y}\text{N}$, which can be determined by the band-gap discontinuity ΔE_C . F in Eq. (5) is the absolute value of the BEF in the strained QW, which can be calculated from Eq. (4). The electron bound state energy E can be obtained by solving

$$[k_R \text{Ai}(t_R) - K \text{Ai}'(t_R)] \cdot [k_L \text{Bi}(t_L) + K \text{Bi}'(t_L)] = [k_L \text{Ai}(t_L) + K \text{Ai}'(t_L)] \cdot [k_R \text{Bi}(t_R) - K \text{Bi}'(t_R)] \quad (7)$$

where

$$t_L = -\left(\frac{2m^*}{\hbar^2} eF \right)^{1/3} \left(\frac{E}{eF} - \frac{L}{2} \right) \quad (8)$$

$$t_R = -\left(\frac{2m^*}{\hbar^2} eF \right)^{1/3} \left(\frac{E}{eF} + \frac{L}{2} \right) \quad (9)$$

$$k_L = \left[\frac{2m^*}{\hbar^2} \left(V_0 + \frac{eFL}{2} - E \right) \right]^{1/2} \quad (10)$$

$$k_R = \left[\frac{2m^*}{\hbar^2} \left(V_0 - \frac{eFL}{2} - E \right) \right]^{1/2} \quad (11)$$

$$K = \left(\frac{2m^*}{\hbar^2} eF \right)^{1/3} \quad (12)$$

The electron wave function in the z direction $\psi(z)$ can be obtained by means of a linear combination of the two independent Airy

functions Ai and Bi ,

$$\psi(z) = \begin{cases} \{\text{Bi}(t_L) - \lambda \text{Ai}(t_L)\} \cdot e^{k_L(z+L/2)}, & z \leq -L/2 \\ \text{Bi}(t) - \lambda \text{Ai}(t), & |z| < L/2 \\ \{\text{Bi}(t_R) - \lambda \text{Ai}(t_R)\} \cdot e^{-k_R(z-L/2)}, & z \geq L/2 \end{cases} \quad (13)$$

where

$$\lambda = \frac{K \text{Bi}'(t_L) + k_L \text{Bi}(t_L)}{K \text{Ai}'(t_L) + k_L \text{Ai}(t_L)} \quad (14)$$

$$t = -\left(\frac{2m^*}{\hbar^2} eF \right)^{1/3} \left(z + \frac{E}{eF} \right) \quad (15)$$

4. Linear and nonlinear intersubband optical absorptions in strained InGaN single QWs

By means of the density matrix method [18,19], the linear and nonlinear intersubband optical absorption coefficients in an $\text{In}_x\text{Ga}_{1-x}\text{N}/\text{Al}_y\text{Ga}_{1-y}\text{N}$ strained QW can be derived as?

$$\alpha^{(1)}(\omega) = \omega \sqrt{\frac{\mu}{\varepsilon_R}} |M_{21}|^2 \left(\frac{m^* k_B T}{L\pi\hbar^2} \right) \cdot \ln \left\{ \frac{1 + \exp[(E_F - E_1)/k_B T]}{1 + \exp[(E_F - E_2)/k_B T]} \right\} \cdot \frac{\hbar/\tau_{in}}{(E_2 - E_1 - \hbar\omega)^2 + (\hbar/\tau_{in})^2} \quad (16)$$

and

where μ is the permeability of the well material, ε_R is the real part of the permittivity, n_r is the refractive index ($\varepsilon_R = n_r^2 \varepsilon_0$), c is the speed of light in free space, E_1 (E_2) is the initial (final) state energy, τ_{in} is the intrasubband relaxation time, ω is the angular frequency of optical radiation, I is the optical intensity, and E_F is the Fermi energy. It is worthwhile to point out that the linear absorption comes from the contribution of the linear susceptibility $\chi^{(1)}$ term and the nonlinearity in the absorption coefficient is due to the third-order nonlinear susceptibility $\chi^{(3)}$ term [20].

For an intersubband optical transition with polarization along z direction, the dipole matrix element can be written as

$$M_{ij} = \langle i | e \cdot z | j \rangle \quad (18)$$

where $|i\rangle$ and $|j\rangle$ denote initial and final states of the optical transition, respectively. Based on Eqs. (16) and (17), the total intersubband optical absorption coefficient $\alpha(\omega, I)$ can be given by

$$\alpha(\omega, I) = \alpha^{(1)}(\omega) + \alpha^{(3)}(\omega, I) \quad (19)$$

Since $\alpha^{(3)}(\omega, I)$ is negative and is proportional to the intensity I , $\alpha(\omega, I)$ decreases as I increases. The absorption coefficient $\alpha(\omega, I)$ is reduced by one-half when I reaches a value I_s called the saturation intensity [20], so we have the following relation:

$$\alpha(\omega, I_s) = \alpha^{(1)}(\omega)/2 \quad (20)$$

or equivalently,

$$\alpha^{(3)}(\omega, I_s) = -\alpha^{(1)}(\omega)/2 \quad (21)$$

5. Numerical results and discussion

We have solved the electron states and calculated the linear and nonlinear intersubband optical absorption coefficients for $\text{In}_x\text{Ga}_{1-x}\text{N}/\text{Al}_y\text{Ga}_{1-y}\text{N}$ strained single QWs. The physical parameters are chosen as follows. The electron effective mass is $m^* = 0.2m_0$ [21]. The real part of the permittivity is chosen to be $\epsilon_R = 10.4$ [21]. The lattice constants are $a = 3.189(1-x) + 3.548x\text{\AA}$ for $\text{In}_x\text{Ga}_{1-x}\text{N}$ [21], and $a = 3.189(1-y) + 3.112y\text{\AA}$ for $\text{Al}_y\text{Ga}_{1-y}\text{N}$ [22]. The band-gap discontinuity is $\Delta E_G = \{3.4(1-y) + 6.2y - y(1-y)\} - \{3.4(1-x) + 1.9x - 3.2x(1-x)\} \text{ eV}$ [17,21,22]. The conduction band offset is chosen as 75% of the total band-gap discontinuity [23]. The spontaneous polarizations are $P_{SP}^{\text{InGa}} = -0.029(1-x) - 0.032xC/\text{m}^2$ for $\text{In}_x\text{Ga}_{1-x}\text{N}$ and $P_{SP}^{\text{AlGa}} = -0.029(1-y) - 0.081yC/\text{m}^2$ for $\text{Al}_y\text{Ga}_{1-y}\text{N}$ [22]. The piezoelectric constants are $e_{31} = -0.2(1-x) - 0.23xC/\text{m}^2$ and $e_{33} = 0.29(1-x) + 0.39xC/\text{m}^2$ [23]. The elastic constants are $C_{13} = 11.4(1-x) + 9.4x$ and $C_{33} = 38.1(1-x) + 20.0x$ in units of 10^{11} dyn/cm^2 [24]. The relaxation time is $\tau_{in} = 0.24 \text{ ps}$ [25].

In order to understand the following results, we should note that, in Section 2, the BEF F has been defined as an electric field induced by the spontaneous polarization of the wurtzite structure and the piezoelectric polarization due to the lattice mismatch between the $\text{In}_x\text{Ga}_{1-x}\text{N}$ and $\text{Al}_y\text{Ga}_{1-y}\text{N}$ layers. Hence the F is not obviously influenced by the electronic charge redistribution or accumulation in the QW. Moreover, following Refs. [18,20,26], the influence of the electronic charge accumulation in the QW on the electron energy level distribution is minor and has been ignored in the present calculations.

Fig. 3 shows our theoretical results of the absorption coefficient α for three different optical intensities. Based on Eq. (20), we can see that the saturated absorption occurs at $I = 25 \text{ MW/cm}^2$. Considering the BEF effect, we calculate the linear absorption coefficient in Fig. 4. For comparison, the result without the BEF effect is also given in Fig. 4. We can easily find that the absorption peak is shifted to a higher energy due to the BEF. The shift of the absorption peak can be explained based on

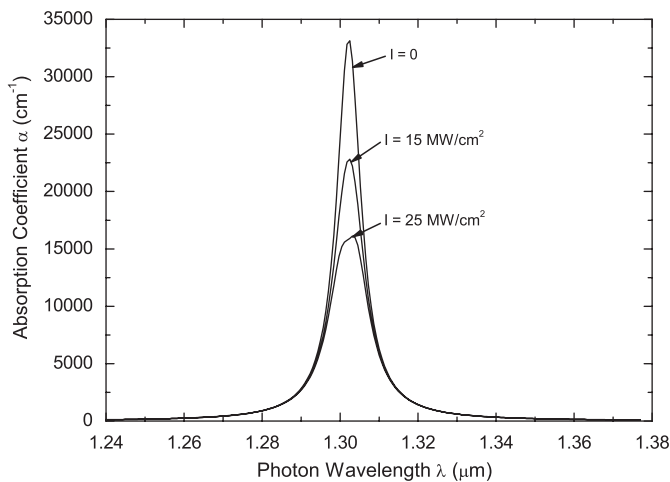


Fig. 3. Intersubband optical absorption coefficient α for an $\text{In}_{0.3}\text{Ga}_{0.7}\text{N}/\text{Al}_{0.6}\text{Ga}_{0.4}\text{N}$ quantum well with the well width $L = 6 \text{ nm}$ for three different optical intensities: (i) $I = 0$, (ii) $I = 15 \text{ MW/cm}^2$, and (iii) $I = 25 \text{ MW/cm}^2$. Here the built-in electric field is considered. The electron density is chosen as $5.0 \times 10^{18} \text{ cm}^{-3}$ and $T = 300 \text{ K}$.

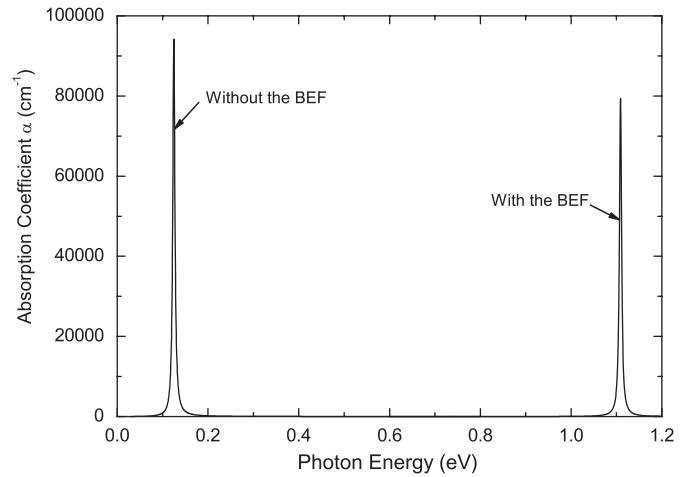


Fig. 4. Linear intersubband optical absorption coefficient α versus photon energy in an $\text{In}_{0.4}\text{Ga}_{0.6}\text{N}/\text{Al}_{0.7}\text{Ga}_{0.3}\text{N}$ quantum well with the well width $L = 6 \text{ nm}$. Here the electron density is chosen as $5.0 \times 10^{18} \text{ cm}^{-3}$ and $T = 300 \text{ K}$.

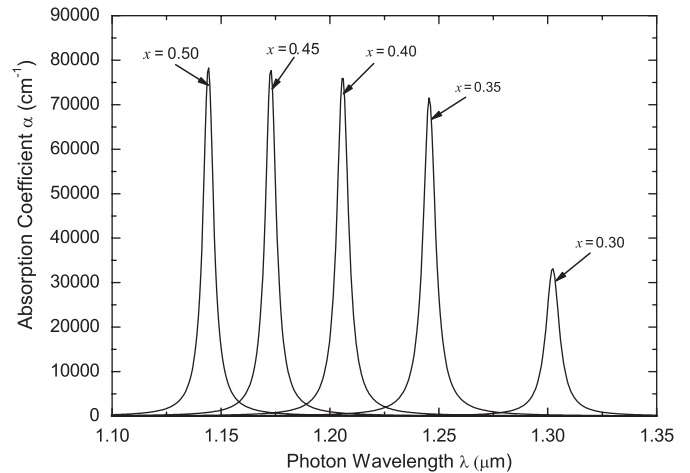


Fig. 5. Linear intersubband optical absorption coefficient α as a function of the photon wavelength in $\text{In}_x\text{Ga}_{1-x}\text{N}/\text{Al}_{0.6}\text{Ga}_{0.4}\text{N}$ QWs with the well width $L = 6 \text{ nm}$. Here the built-in electric field is included. The electron density is chosen as $5.0 \times 10^{18} \text{ cm}^{-3}$ and $T = 300 \text{ K}$. Five different In compositions are considered: (i) $x = 0.30$, (ii) $x = 0.35$, (iii) $x = 0.40$, (iv) $x = 0.45$, and (v) $x = 0.50$.

the quantum confined Stark effect induced by the BEF (refer to Fig. 2).

In order to investigate the influence of the well depth on the intersubband optical absorption, we calculate the linear absorption coefficient for different In (Al) fraction x (y) in the $\text{In}_x\text{Ga}_{1-x}\text{N}/\text{Al}_y\text{Ga}_{1-y}\text{N}$ strained single QWs. We can find from Figs. 5 and 6 that the peak wavelength of the intersubband optical absorptions decreases if the In (Al) composition increases. The physical reason can be understood as follows. If In fraction x increases, the BEF becomes much stronger (refer to Fig. 1) and the potential well is much deeper. The energy difference between the two confined electron states increases. If Al composition y increases, the QW depth becomes much deeper. Similarly, the energy difference between the two confined electron states becomes larger. The absorption peak will thus be moved to a higher energy. The results of Figs. 5 and 6 are useful for designing electro-optical modulators and photodetectors in the near-infrared region.

Fig. 7 indicates the calculated linear absorption coefficient α for the $\text{In}_{0.3}\text{Ga}_{0.7}\text{N}/\text{Al}_{0.6}\text{Ga}_{0.4}\text{N}$ QW with different electron concentrations. We can find from Fig. 7 that the value of the absorption peak is enhanced if the electron density increases. This can be

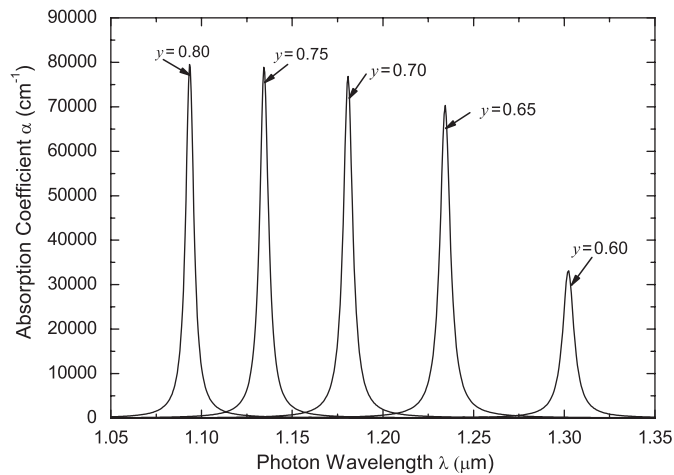


Fig. 6. Linear intersubband optical absorption coefficient α as a function of the photon wavelength in $\text{In}_{0.3}\text{Ga}_{0.7}\text{N}/\text{Al}_y\text{Ga}_{1-y}\text{N}$ QWs with the well width $L = 6$ nm. Here the built-in electric field is included. The electron density is chosen as $5.0 \times 10^{18} \text{ cm}^{-3}$ and $T = 300$ K. Five different Al compositions are considered: (i) $y = 0.60$, (ii) $y = 0.65$, (iii) $y = 0.70$, (iv) $y = 0.75$, and (v) $y = 0.80$.

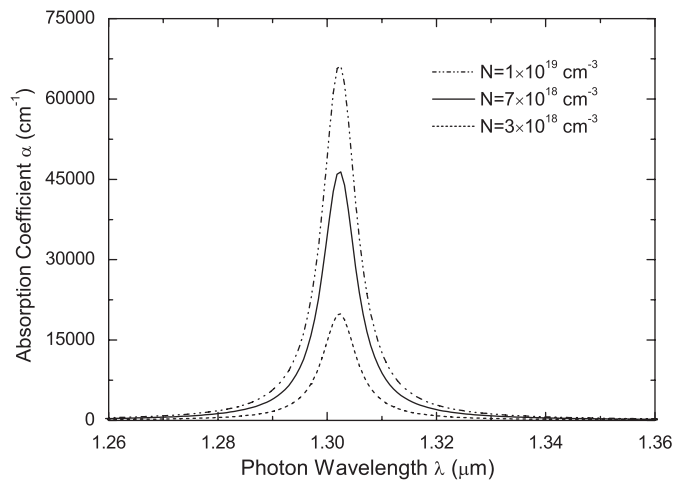


Fig. 7. Linear intersubband optical absorption coefficient α as a function of the photon wavelength in an $\text{In}_{0.3}\text{Ga}_{0.7}\text{N}/\text{Al}_{0.6}\text{Ga}_{0.4}\text{N}$ QW with the well width $L = 6$ nm at $T = 300$ K. Here the built-in electric field is considered. Three different electron densities are chosen: (i) $3.0 \times 10^{18} \text{ cm}^{-3}$, (ii) $7.0 \times 10^{18} \text{ cm}^{-3}$, and (iii) $1.0 \times 10^{19} \text{ cm}^{-3}$.

completely understood based on Eqs. (5) and (16). The physical reason is because the Fermi level increases with the electron density increasing. The matrix element $|M_{21}|$ and the initial (final) state energy E_1 (E_2) are invariable due to a constant BEF F (see the above analysis). Hence the magnitude of the absorption peak should increase if increasing the electron density, as shown in Fig. 7.

6. Conclusions

In conclusion, we have calculated the BEF in wurtzite $\text{In}_x\text{Ga}_{1-x}\text{N}/\text{Al}_y\text{Ga}_{1-y}\text{N}$ strained single QWs with a thin $\text{In}_x\text{Ga}_{1-x}\text{N}$ strained layer sandwiched between the two thick $\text{Al}_y\text{Ga}_{1-y}\text{N}$

layers. We find that the BEF is very strong, of the order of MV/cm. The increase of the In composition will enhance the strength of the BEF. Considering the strong BEF effect, we further calculate the linear and nonlinear intersubband optical absorption coefficients by using the density matrix method. Our results show that the position of the absorption peak has a great blue shift due to the strong BEF. Moreover, we find that the saturated absorption can be obtained when $I = 25 \text{ MW/cm}^2$ for an $\text{In}_{0.3}\text{Ga}_{0.7}\text{N}/\text{Al}_{0.6}\text{Ga}_{0.4}\text{N}$ QW with the well width $L = 6$ nm if choosing electron density as $5.0 \times 10^{18} \text{ cm}^{-3}$ and $T = 300$ K. The increase of the compositions of In and Al reduces the peak absorption wavelength. The magnitude of the optical absorption coefficient increases if the electron density increases. Based on the present results, we hope that the important infrared photodetectors and near-infrared laser amplifiers can be constructed based on the group-III nitride QWs.

Acknowledgments

This work was funded jointly by the National Basic Research Program of China under Grant no. 2006CB921607 and the China-Australia special fund of the National Natural Science Foundation of China for science and technology under Grant no. 60711120203.

References

- [1] S. Nakamura, M. Senoh, S. Nagahama, N. Iwasa, T. Yamada, T. Matsushita, H. Kiyoku, Y. Sugimoto, T. Kozaki, H. Umemoto, M. Sano, K. Chocho, Appl. Phys. Lett. 73 (1998) 832.
- [2] S. Nakamura, S.F. Chichibu, Introduction to Nitride Semiconductor Blue Lasers and Light Emitting Diodes, Taylor & Francis, London, 2000.
- [3] C. Gmachl, H.M. Ng, A.Y. Cho, Appl. Phys. Lett. 77 (2000) 334.
- [4] D. Hofstetter, L. Diehl, J. Faist, W.J. Schaff, J. Hwang, L.F. Eastman, C. Zellweger, Appl. Phys. Lett. 80 (2002) 2991.
- [5] B.K. Ridley, W.J. Schaff, L.F. Eastman, J. Appl. Phys. 94 (2003) 3972.
- [6] M. Tchernycheva, L. Nevou, L. Doyennette, F.H. Julien, E. Warde, F. Guillot, E. Monroy, E. Bellet-Amalric, T. Remmele, M. Albrecht, Phys. Rev. B 73 (2006) 125347.
- [7] C. Gmachl, H.M. Ng, S.-N.G. Chu, Appl. Phys. Lett. 77 (2000) 3722.
- [8] N. Iizuka, K. Kaneko, N. Suzuki, T. Asano, S. Noda, O. Wada, Appl. Phys. Lett. 77 (2000) 648.
- [9] N. Iizuka, K. Kaneko, N. Suzuki, Appl. Phys. Lett. 81 (2002) 1803.
- [10] S.Y. Lei, B. Shen, L. Cao, F.J. Xu, Z.J. Yang, K. Xu, G.Y. Zhang, J. Appl. Phys. 99 (2006) 074501.
- [11] S. Ünlü, İ. Karabulut, H. Şafak, Physica E 33 (2006) 319.
- [12] P. Waltereit, M.D. Craven, S.P. DenBaars, J.S. Speck, J. Appl. Phys. 92 (2002) 456.
- [13] F. Bernardini, V. Fiorentini, D. Vanderbilt, Phys. Rev. Lett. 79 (1997) 3958.
- [14] J.J. Shi, Solid State Commun. 124 (2002) 341.
- [15] V. Jovanović, D. Indjin, Z. Ikonić, V. Milanović, J. Radovanović, Solid State Commun. 121 (2002) 619.
- [16] F. Bernardini, V. Fiorentini, D. Vanderbilt, Phys. Rev. B 56 (1997) R10024.
- [17] T. Takeuchi, S. Sota, M. Katsuragawa, M. Komori, H. Takeuchi, H. Amano, I. Akasaki, Jpn. J. Appl. Phys. 36 (Part 2) (1997) L382.
- [18] S.H. Pan, S.M. Feng, Phys. Rev. B 44 (1991) 8165.
- [19] J.J. Shi, E.M. Goldys, IEEE Trans. Electron Devices 46 (1999) 83.
- [20] İ. Karabulut, Ü. Atav, H. Şafak, M. Tomak, Eur. Phys. J. B 55 (2007) 283.
- [21] T. Takeuchi, H. Amano, I. Akasaki, Jpn. J. Appl. Phys. 39 (Part 1) (2000) L413.
- [22] I. Vurgaftman, J.R. Meyer, L.R. Ram-Mohan, Appl. Phys. Lett. 89 (2001) 5815.
- [23] T. Takeuchi, C. Wetzel, S. Yamaguchi, H. Sakai, H. Amano, I. Akasaki, Y. Kaneko, Y. Yamaoka, S. Nakagawa, N. Yamada, Appl. Phys. Lett. 73 (1998) 1691.
- [24] M. Yamaguchi, T. Yagi, T. Azuhata, T. Sota, K. Suzuki, S. Chichibu, S. Nakamura, J. Phys.: Condens. Matter 9 (1997) 241.
- [25] S.-H. Park, D. Ahn, E.H. Par, T.K. Yoo, Appl. Phys. Lett. 87 (2005) 044103.
- [26] D. Ahn, S.L. Chuang, IEEE J. Quantum Electron. QE-23 (1987) 2196.